

Particle characterization for additive manufacturing: Analysis of the key parameters particle size and shape using only one instrument

Dr. Frederik Schleife (frederik.schleife@3P-instruments.com), Dr. Christian Oetzel
3P Instruments GmbH & Co. KG, www.3P-instruments.com

1. Introduction and objectives

Additive manufacturing (AM) processes can be used to produce very complex components in a precise and customized manner. Compared to conventional manufacturing processes, in which components are produced by removing excess material (*top-down* approach, e.g., turning, milling, grinding), additive manufacturing uses the so-called *bottom-up* approach. In this case, the desired workpieces are built up three-dimensionally layer by layer. This can be achieved in various ways, such as selective melting or sintering of a powder using laser or electron beams, extrusion and deposition of heated polymers or selective curing of photoactive polymers. Regardless of the selected method, additive manufacturing can be used to realize structures that would not be possible using traditional material removal processes. Another decisive advantage of AM processes lies in the short manufacturing chain between digital design and finished workpiece ^[1]. The information for manufacturing a specific workpiece is imported into the manufacturing machines as digital file. This allows the same component to be manufactured at different locations without any problems, even with tight specifications, since only the production machine, the digital information on the workpiece, and the raw material are required. This eliminates the need for supply chains of, for example, preliminary stages or finished workpieces, which contributes to time-efficient and more cost-effective production.

The final product properties of workpieces manufactured by means of additive manufacturing are essentially

influenced by the starting material and its powder properties ^[2]. The most important characteristics are particle size distribution ^[3], particle shape ^{[3] [4]}, chemical composition ^{[5] [6]}, flowability ^[7] powder layer density (*PLD*) ^[8] ^[9], and internal porosity ^[3]. Nevertheless, there are currently no quantified or specified and widely accepted parameters for describing powder properties for the use in additive manufacturing ^[4], or they are kept secret by powder manufacturers for competitive reasons ^[2]. Thus, the monitoring of raw material quality is more than essential for additive manufacturing to ensure consistent product properties.

Another interesting correlation between the influence of powder characteristics on the final properties of the workpiece produced, for example, by laser beam melting (*LBM - Laser Beam Melting/SLM - Selective Laser Melting*) arises from the question of whether powder fed into the process but not melted must be discarded or can be reused for production ^[10]. Since the production volume of components manufactured by laser melting is continuously increasing ^[11] and the majority of the powder used (95-97 % ^[12]) is not melted, this question should be answered from both economic and ecological aspects.

During the LBM process, so-called *spatter particles* are formed, which are deposited in the powder bed and in the production zone of the LBM machine and thus accumulate in the recycling powder ^[13]. It is also known that a higher energy density of the laser radiation used leads to an increase in the formation of spatter particles ^{[14] [15]}.

Although the influence of the spatter particles on the final product quality of the manufactured workpiece needs to be further investigated, the analysis of the particle size distribution and particle shape of the fresh powder compared to the spatter particles is a crucial approach ^[10].

In addition to the classical method of laser diffraction (static laser light scattering) for the determination of the particle size distribution, an imaging method is needed for the acquisition of the shape factors of particle collectives and especially of single particles. In this context, dynamic image analysis is excellent in providing statistics and thus representative analysis of the mean particle shape parameters of the entire collective due to the rapid capture of many individual particles. In addition, single particle acquisition allows the detection and analysis of statistically underrepresented oversized particles or fractions of heterogeneous powder samples with respect to size and/or shape.

The Bettersizer S3 Plus (Fig. 1) is a measuring instrument that uniquely allows the analysis of particle size distribution from the nano to the millimeter range by means of classical laser diffraction and the simultaneous characterization of particle shape as well as oversize and agglomeration phenomena by means of dynamic image analysis.



Figure 1 *Bettersizer S3 Plus: combination of laser diffraction and dynamic image analysis*

2. The Bettersizer S3 Plus: one instrument, two essential powder properties

Fig. 2 shows the optical unit of the Bettersizer S3 Plus: the wet measuring cell is located in the center of the main platform, two Fourier lenses are placed directly to the right and left of the cell (two Fourier lenses = dual lens technology). To the right of the measuring cell is the laser light source arranged at an angle (green DPSS laser, wavelength = 532 nm), directed perpendicular to the

measuring cell is the CCD camera system (two cameras with different lenses: 0.5x and 10x) and the backscattering detectors.

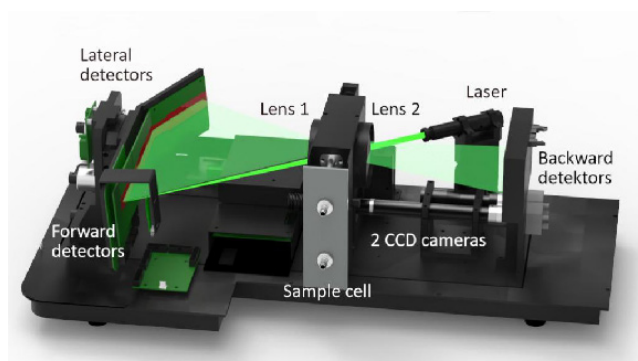


Figure 2 *Setup of the Bettersizer S3 Plus incl. dual lens system with DLOI (Dual Lenses & Oblique Incidence) System technology and CCD camera unit (0.5x and 10x)*

To the left of the measuring cell, the detector system for detecting forward and side scattering is installed. This special setup enables:

1. The exact measurement of very small particles (from 10 nm) using the double lens technique (static laser light scattering, see section 2.1).
2. At the same time, highest measuring precision for very coarse particles (up to 3.5 mm), optionally supported by the 0.5x CCD camera (static laser light scattering combined with dynamic image analysis).
3. Particle shape determination, oversized particle analysis and agglomerate check with the 0.5x and/or 10x CCD camera (dynamic image analysis, see section 2.2).

2.1. Laser diffraction/static laser light scattering with the innovative double lens technique (DLOI System)

Fig. 2 shows the schematic diagram of the Bettersizer S3 Plus: the special feature of this laser setup is the DLOI System technology (= **D**ual **L**enses & **O**blique **I**ncidence). The laser is arranged inclined to the measuring cuvette to allow the widest possible scattering angle range of the lateral front detectors. Fourier Lens 2 produces an exact parallel laser beam that impinges on the sample. Lens 1 focuses the scattered light into the detector plane according to the known Fourier setup, thus the scattering particles in the cuvette do not necessarily have to lie in one plane - a decisive advantage over the conventional reverse Fourier setup ^[16]. Lens 2, in turn, ensures focusing and thus detection of the backscattered radiation, yielding

a very large angular range (0.02 - 165°) with excellent detector resolution compared to other systems on the market. In particular, a high scattered light resolution in the backscattering range (> 90°) is crucial for the accurate detection of very small particles (< approx. 500 nm) [16].

The extremely wide angular coverage also has the advantage that a second, shorter-wavelength laser can be avoided. Accordingly, no scattering spectra of mixed wavelengths are measured, which is advantageous as the evaluation of those spectra is strictly speaking not allowed using the commonly used models (Fraunhofer and Mie).

2.2. Dynamic image analysis for particle shape analysis

Depending on the distribution range of the sample to be analyzed, the two high-speed CCD cameras of the Bettersizer S3 Plus can be used either individually or in combination for comprehensive particle size and shape analysis solely based on dynamic image analysis. The according size range is

- a) 30 – 3,500 µm for the 0.5x camera
- b) 4 – 100 µm for the 10x camera

Depending on the particle size and sample concentration, several thousand to several 100,000 particles can be recorded per minute with both cameras. For very broad distributions, the combined use of both cameras is recommended.

During the analysis, each individual particle is captured in real time, stored as an image, numbered and statistically evaluated [17]. In addition to various equivalent diameters (e.g., area, perimeter, maximum and minimum Feret), special shape parameters such as aspect ratio, length L/width D, circularity (roundness), convexity, perimeter and many more are calculated [18].

Particularly in the case of strongly shape-anisotropic particles such as fibers or platelets, this is a clear advantage over classical, "pure" laser diffraction, which assumes spherical particles during evaluation. In addition, the degree of agglomeration of the systems can be assessed and special tasks such as oversize particle analysis can be realized. The determination of different equivalent diameters also offers the possibility to compare with other methods for size determination, such as sieving, and to verify their measurement results.

3. Application example: the particulate properties of a fresh AlSi10Mg powder compared to the powder recovered after the LBM process

In order to illustrate the advantages of the Bettersizer S3 Plus for the quality assessment of powder samples for additive manufacturing using an application-related example, two different AlSi10Mg samples were examined with regard to their particle size distribution and particle shape. The sample *AlSi10Mg fresh* was a fresh powder, as received from the supplier. This was fed to an SLM manufacturing machine. After the production step, the sample *AlSi10Mg spatter particles* was recovered from the fabrication zone of the SLM machine. Both powder samples were dispersed separately in ethanol and characterized using the Bettersizer S3 Plus with respect to particle size distribution by classical laser diffraction and particle shape by dynamic image analysis. For this purpose, the powder samples were added to the ethanol-filled dispersion unit of the Bettersizer S3 Plus and pretreated with the device's internal ultrasonic dispersion for one minute before measurement.

Tab. 1 shows the characteristic diameters of the volume-based particle size distributions obtained by laser diffraction. In Fig. 3, the superimposed distribution functions are shown graphically in the form of the histograms and the cumulative curves.

Table 1 Characteristic diameters of the volume-based particle size distributions of the investigated samples obtained by laser diffraction

Sample	D10 / µm	D50 / µm	D90 / µm	D97 / µm	SPAN
AlSi10Mg fresh	27.08	44.39	71.10	86.72	0.991
AlSi10Mg spatter particles	36.20	62.89	106.4	131.7	1.117

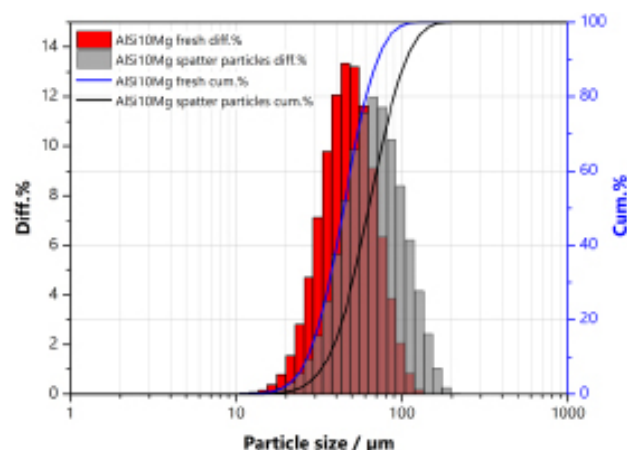


Figure 3 Superposition of the volume-based particle size distributions of the investigated samples obtained by laser diffraction

From the measurement results of the laser diffraction experiments, it is clear that the spatter particles have a coarser particle size distribution compared to the fresh AISi10Mg sample. Likewise, from the SPAN values determined ($= (D_{90} - D_{10}) / D_{50}$), it is evident that the *AISI10Mg spatter particles* have a broader distribution than *AISI10Mg fresh*.

For the evaluation of the particle shape, a representative number of individual particles were recorded from both samples with the high-speed CCD cameras of the Bettersizer S3 Plus and were evaluated number-based with respect to the ISO shape parameters circularity and aspect ratio. The characteristic values of the distribution functions of both shape parameters are summarized in Tab. 2 and superimposed in Figs. 4 and 5. Tab. 3 and 4 list selected individual particle parameters of the six largest particles detected with the 10x camera of the Bettersizer S3 Plus and show their appearance.

Table 2 Characteristic % values of the number-based particle shape distributions of the investigated samples obtained by dynamic image analysis

Sample	Number of detected particles	Parameter	x1	x10	x50	x90	x99
AISI10Mg fresh	3,909	Circularity	0.739	0.839	0.904	0.933	0.945
		Aspect ratio	0.425	0.608	0.866	0.975	1.000
AISI10Mg spatter particles	2,909	Circularity	0.782	0.861	0.917	0.938	0.947
		Aspect ratio	0.487	0.672	0.916	0.983	1.000

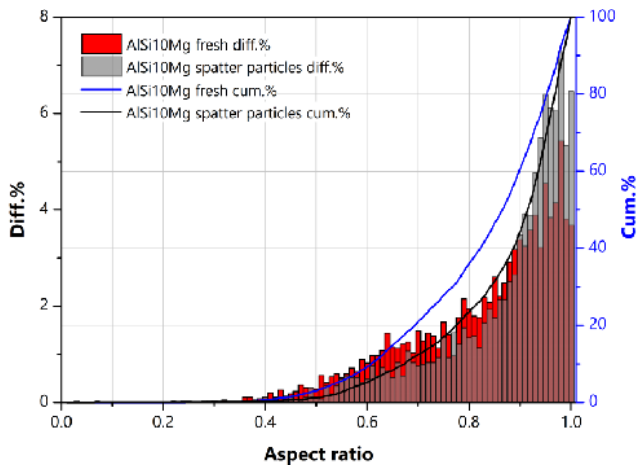


Figure 4 Superposition of the number-based distribution functions of the aspect ratio of the studied samples

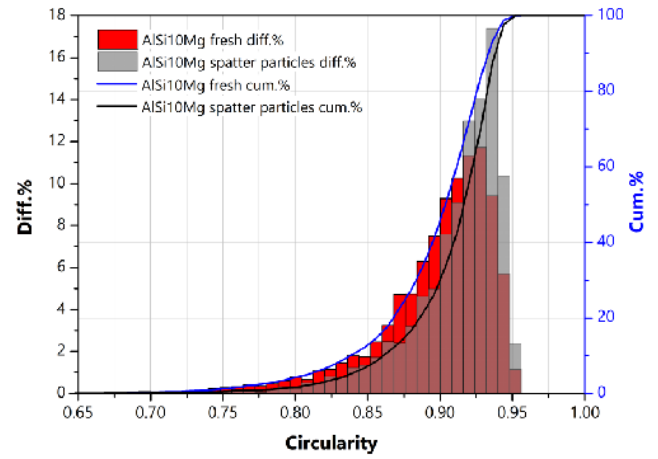


Figure 5 Superposition of the number-based distribution functions of the circularity of the studied samples

Table 3 Selected single particle parameters of the 6 largest particles of the sample AISi10Mg fresh detected by the 10x camera

No.	Area / μm^2	CE diameter / μm	Length / μm	Width / μm	Circularity	Convexity	Aspect ratio	Image
1	6,600	91.67	139.3	62.87	0.771	0.892	0.451	
2	6,069	87.91	128.7	61.40	0.801	0.920	0.476	
3	5,632	84.68	121.2	61.55	0.767	0.876	0.507	
4	5,303	82.17	105.5	71.61	0.755	0.868	0.678	
5	5,021	79.95	125.8	53.53	0.737	0.888	0.425	
6	5,017	79.92	94.07	70.70	0.833	0.885	0.751	

Table 4 Selected single particle parameters of the 6 largest particles of the sample AISi10Mg spatter particles detected by the 10x camera

No.	Area / μm^2	CE diameter / μm	Length / μm	Width / μm	Circularity	Convexity	Aspect ratio	Image
1	20,049	159.7	162.3	154.6	0.862	0.886	0.952	
2	16,984	147.0	168.7	132.1	0.912	0.938	0.783	
3	13,117	129.2	132.3	128.9	0.903	0.924	0.974	
4	11,470	120.8	122.7	116.9	0.854	0.888	0.953	
5	11,237	119.6	120.8	113.5	0.907	0.938	0.940	
6	10,863	117.6	134.0	108.0	0.835	0.871	0.805	

The results of the dynamic image analyses on both samples, as well as their comparison with each other, show a significantly larger aspect ratio and thus a lower average expansion of the spatter particles (sample *AISI10Mg spatter particles*) compared to the particles of the unused powder sample *AISI10Mg fresh*. Likewise, the spatter particles exhibit higher mean circularity and are thus characterized by lower shape anisotropy (resp. higher sphericity) than the particles before being used in the AM process.

4. Summary and conclusion

Based on the investigations carried out with the Bettersizer S3 Plus, both samples analyzed in terms of particle size and shape can be clearly distinguished from each other. The findings that the *spatter particles* recovered after the additive manufacturing process are characterized by a coarser and more widely distributed particle size and higher sphericity compared to the *fresh AlSi10Mg* particles are in line with observations known from the literature [10]. This shows that the Bettersizer S3 Plus is perfectly suitable for the quality control of raw materials for additive manufacturing processes, and also makes a significant contribution to a better understanding of the influences on the final product properties of the workpieces produced by additive manufacturing from a research and development perspective. This is essentially due to the unique combination of the laser diffraction and dynamic image analysis measurement methods in one measuring device. This enables a fast, simple and cost-efficient analysis of the powder raw materials.

For the final answer to the question of whether a recovered powder is appropriate for reuse in additive manufacturing or whether it must be subjected to further preparative steps (sieving, purification, mixing with fresh powder), additional investigations are necessary. A chemical analysis of the alloy composition and an assessment of the quality of workpieces produced using recovered powder are essential.

5. Acknowledgement

We would like to thank Prof. Dr.-Ing. Vesna Nedeljkovic-Groha and Dipl.-Ing. Stefan Brenner of the Faculty of Mechanical Engineering at the *Universität der Bundeswehr München* for kindly providing the samples as well as advice and explanations on the application side.

Literature

[1] J. A. Slotwinski, E. J. Garboczi, P. E. Stutzman, C. F. Ferraris, S. S. Watson und M. A. Peltz, „Characterization of Metal Powders Used for Additive Manufacturing,” *Journal of Research of the National Institute of Standards and Technology*, Bd. 119, p. 460, 2014.

[2] L. Haferkamp, L. Haudenschild, A. Spierings, K.

Wegener, K. Riener, S. Ziegelmeier und G. J. Leichtfried, „The Influence of Particle Shape, Powder Flowability, and Powder Layer Density on Part Density in Laser Powder Bed Fusion,” *Metals*, Bd. 11, Nr. 3, p. 418, 2021.

[3] W. J. Sames, F. A. List, S. Pannala, R. R. Dehoff und S. S. Babu, „The metallurgy and processing science of metal additive manufacturing,” *Int. Mater. Rev.*, Bd. 61, p. 315, 2016.

[4] J. H. Tan, W. L. Wong und K. W. Dalgarno, „An overview of powder granulometry on feedstock and part performance in the selective laser melting process,” *Addit. Manuf.*, Bd. 18, p. 228, 2017.

[5] R. Engeli, T. Etter, S. Hövel und K. Wegener, „Processability of different IN738LC powder batches by selective laser melting,” *J. Mater. Process. Technol.*, Bd. 229, p. 484, 2016.

[6] J. A. Slotwinski und E. J. Garboczi, „Metrology Needs for Metal Additive Manufacturing Powders,” *J. Mater.*, Bd. 67, p. 538, 2015.

[7] A. B. Spierings, M. Voegtlin, T. Bauer und K. Wegener, „Powder flowability characterisation methodology for powder-bed-based metal additive manufacturing,” *Prog. Addit. Manuf.*, Bd. 1, p. 9, 2016.

[8] T. M. Wischeropp, C. Emmelmann, M. Brandt und A. Pateras, „Measurement of actual powder layer height and packing density in a single layer in selective laser melting,” *Addit. Manuf.*, Bd. 28, p. 176, 2019.

[9] Y. Mahmoodkhani, U. Ali, S. Imani Shahabad, A. Rani Kasinathan, R. Esmaeilzadeh, A. Keshavarzkermani, E. Marzbanrad und E. Toyserkani, „On the measurement of effective powder layer thickness in laser powder-bed fusion additive manufacturing of metals,” *Prog. Addit. Manuf.*, Bd. 4, p. 109, 2019.

[10] M. Lutter-Günther, M. Bröker, T. Mayer, S. Lizak, C. Seidel und G. Reinhart, „Spatter formation during laser beam melting of AlSi10Mg and effects on powder quality,” *Procedia CIRP*, Bd. 74, p. 33, 2018.

[11] T. Wohlers, „3D printing and additive manufacturing state of the industry: annual worldwide progress report,” *Wohlers Report*, 2017.

[12] B. A. Hann, „Powder Reuse and Its Effects on Laser Based Powder Fusion Additive Manufactured Alloy 718,” in

SAE 2016 Aerospace Systems and Technology Conference, Warrendale, PA, 2016.

[13] Y. Liu, Y. Yang, S. Mai, D. Wang und C. Song, „Investigation into spatter behavior during selective laser melting of AlSi 316L stainless steel powder,“ Materials & Design, Bd. 87, p. 797, 2015.

[14] D. Wang, S. Wu, F. Fu, S. Mai, Y. Yang, Y. Liu und C. Song, „Mechanisms and characteristics of spatter generation in SLM processing and its effect on the properties,“ Material & Design, Bd. 117, p. 121, 2017.

[15] M. Taheri Andani, R. Dehghani, M. R. Karamooz-Ravari, R. Mirzaeifar und J. Ni, „A study on the effect of energy input on spatter particles creation during selective laser melting process,“ Addit. Manuf., Bd. 20, p. 33, 2018.

[16] ISO 13320:2020-01, Particle size analysis - Laser diffraction methods, 2020.

[17] ISO 13322-2:2006-11, Particle size analysis - Image analysis methods - Part 2: Dynamic image analysis methods, 2006.

[18] ISO 9276-6:2008-09, Representation of results of particle size analysis - Part 6: Descriptive and quantitative representation of particle shape and morphology, 2008.



Betersize Instruments Ltd.

Further information can be found at

<https://www.betersizeinstruments.com>

Email: info@betersize.com

Address: No. 9, Ganquan Road, Lingang Industrial Park, Dandong, Liaoning, China

Postcode: 118009

Tel: +86-415-6163800

Fax: +86-415-6170645

Download Our Application Notes:



Visit Our Betersizer S3 Plus Site:

